Clinical characterization of *CNGB1* related autosomal recessive retinitis pigmentosa

Sarah Hull MA, FRCOphth, PhD [*1, 2]; Marcella Attanasio MD [*,1,3]; Gavin Arno PhD [1, 2]; Keren Carss PhD[4, 5]; Anthony G. Robson, MSc, PhD[1,2]; Dorothy A Thompson MCOptom, PhD[6]; Vincent Plagnol MSc, PhD[7]; Michel Michaelides MD(res), FRCOphth[1, 2]; Graham E Holder MSc, PhD [1, 2]; Robert H Henderson MD(Res), FRCOphth[1,6]; F Lucy Raymond MA, D Phil, FRCP[5,7]; Anthony T Moore MA, FRCOphth[1,2,9] ; Andrew R Webster MD(res), FRCOphth [1, 2]

* These authors contributed equally to this work

[1] Moorfields Eye Hospital, London, UK

[2] University College London Institute of Ophthalmology, London, UK

[3] Ospedale Sacrocuore-Don Calabria, Negrar, Italy

[4] Department of Haematology, University of Cambridge Cambridge, UK

[5] NIHR BioResource - Rare Diseases, Cambridge University Hospitals, Cambridge Biomedical Campus, Cambridge, United Kingdom

[6] Ophthalmology, Great Ormond Street Hospital for Children, London, UK

[7] University College London Genetics Institute, London, UK

[8] Department of Medical Genetics, Cambridge Institute for Medical Research, University of Cambridge Cambridge, UK

[9] Ophthalmology Department University of California San Francisco Medical School, San Francisco, USA

ADDRESS FOR CORRESPONDENCE: Prof Andrew Webster, UCL Institute of Ophthalmology, 11-43 Bath St, London, EC1V 9EL, UK. Tel: 0044 207566 2260. Email: Andrew.webster@ucl.ac.uk

RUNNING HEAD: *CNGB1* related retinitis pigmentosa

Abstract word count: 348

Text word count: 2947

KEY POINTS:

Question: What can a detailed clinical and molecular genetic study of patients with CNGB1-related retinitis pigmentosa reveal about the disease presentation and progression?

Findings: This case series of 10 patients identified childhood onset of nyctalopia with preserved visual acuity and central photoreceptors into adulthood.

Meaning: This case series suggests RP due to variants in CNGB1 is slowly progressive with a long potential treatment window.

Abstract

IMPORTANCE: There is limited published data on the phenotype of retinitis pigmentosa (RP) related to *CNGB1* variants. These data are needed both for prognostic counseling of patients and for understanding potential treatment windows.

OBJECTIVE: To describe the detailed clinical and molecular genetic findings in a series of RP patients with likely pathogenic variants in *CNGB1*.

DESIGN, SETTING AND PARTICIPANTS: Ten patients from nine families underwent full ophthalmologic examination. Molecular investigations included whole exome analysis in 6 patients. The study was conducted from April 17, 2013 to March 3, 2016 with final follow-up completed on March 2, 2016 and data analyzed from October 27, 2014 to March 29, 2016.

MAIN OUTCOMES: Results of ophthalmologic examination and molecular genetic analysis of *CNGB1*.

RESULTS: Seven females and three males from 9 families with a mean age of 47.4 ± 13.2 years old were included in this study having been identified to have *CNGB1* variants; there was a mean follow-up length of 3.7 ± 2.8 years. The first clinical presentation was with nyctalopia in childhood with visual field loss documented later at a mean age of 33.2 ± 8.0 years. All patients had preserved visual acuity into adulthood with a mean of 0.1 LogMAR, Snellen equivalent 20/25 in each eye (range 0 to 0.3, Snellen 20/20 to 20/40 in the right eye and -0.1 to 0.3, Snellen 20/16 to 20/40 in the left eye). Fundus examination revealed mid-peripheral retinal pigment epithelial atrophy and intra-retinal pigment migration. Optical coherence tomography of the macula demonstrated complete preservation of the inner segment ellipsoid band in one patient with variable lateral extent in others, corresponding with the diameter of a paracentral ring of increased fundus autofluorescence. Electrophysiological testing in 6 patients confirmed a rod-cone dystrophy phenotype. Molecular investigations identified a previously reported missense variant (p.N986I) and 7 variants not previously reported in disease including 4 nonsense (p.(Q88*), p.(Q222*), p.(Q318*), p.(R729*)), 2 frameshift (p.(A1048fs*13), p.(L849Afs*3)) and a splice site variant (c.761+2T>A).

CONCLUSIONS AND RELEVANCE: These data suggest that visual acuity and foveal structure are preserved into adult life such that a lengthy window of opportunity should exist for intervention with novel therapies."

Introduction

Retinitis Pigmentosa (RP) is an inherited disorder characterized by a progressive retinal dystrophy with primarily rod photoreceptor dysfunction at presentation. It is highly heterogeneous and affects about 1 in 4000 individuals worldwide.[1-4] Clinically, RP is characterized by night blindness, progressive constriction of peripheral visual fields and ultimately, in the majority of patients, reduced visual acuity. The fundus typically shows mid-peripheral intra-retinal pigment migration associated with retinal pigment epithelium (RPE) atrophy, attenuated retinal vessels and pallor of the optic nerve head.[4-6]

Approximately 15–20% of cases are autosomal dominant, 15% recessive, 7% are X-linked, 43% are sporadic/simplex cases the majority of which are most likely to be autosomal recessive and 15% are unknown.[6,7] Rarely, RP may be caused by mutations in mitochondrial DNA.[4] Genes associated with RP encode proteins that have a key role in retinal structure and function including phototransduction or the visual cycle. Some are ubiquitously expressed but have a phenotype confined to the eye. [6,8,9]

Variants in genes encoding the two rod cyclic nucleotide-gated (CNG) channel subunits have been associated with arRP.[8,10] CNG channels are non-selective cation channels localized to the plasma membrane of rod and cone photoreceptors which translate light-mediated changes of second messenger cyclic guanosine monophosphate (cGMP) into voltage signals.[11,12] CNG channels in rods form heterotetramers consisting of three α-subunits (CNGA1) and one β-subunit (CNGB1); whereas the cone channel is formed by two α-subunits (CNGA3) and two β-subunit (CNGB3).[13,14] Variants in *CNGB1* are an uncommon cause of RP, accounting for approximately 4% of arRP cases; there are limited reports describing the associated phenotypes.[10,15-20] The present report describes the detailed clinical features of ten affected patients harboring likely pathogenic variants in *CNGB1*.

Materials and Methods:

Patients

Ten patients from nine families were ascertained from the inherited retinal clinics of Moorfields Eye Hospital and Great Ormond Street Hospital for Children. Informed written consent and peripheral blood samples were obtained for genetic analysis from all subjects according to approved protocols of the Research Management Committees of Moorfields Eye Hospital and Great Ormond Street Hospital for Children, in agreement with the Declaration of Helsinki.

An accurate family history of each patient was recorded and all underwent a complete ophthalmic examination, which included best-corrected visual acuity (BCVA), slit-lamp biomicroscopy of the anterior segment and dilated fundus examination. Retinal fundus photographs were obtained by conventional 35° fundus color photographs (Topcon Great Britain Ltd) and in one patient by ultra-widefield (up to 200°) confocal laser scanning ophthalmoscopy (Optos plc, Dunfermline, Scotland). FAF imaging (30° and 55°) was performed with a confocal scanning laser ophthalmoscope (OCT-SLO Spectralis, Heidelberg Retina Angiograph 2, Heidelberg Engineering, Dossenheim, Germany). An optically pumped solid-state laser (488 nm) was used for excitation and a 500 nm barrier filter was used to modulate the reflected light. Spectral-domain OCT was performed with the OCT-SLO Spectralis, Heidelberg Retina Angiograph (Heidelberg Engineering, Dossenheim, Germany). OCT imaging was acquired by a broadband 870-nm superluminescent diode that scanned the retina at 40,000 A-scans per second with an optical depth resolution of 7 μm. In particular, the central subfield thickness (CST) and morphology of the inner segment ellipsoid (ISe) band of the photoreceptors were assessed in the maculae of both eyes of all patients. CST was measured using the automated Heidelberg Spectralis viewing module (version 6.3.4.0) with slices visually inspected for segmentation accuracy.

Full-field electroretinography (ERG, 6 patients) and pattern electroretinography (PERG, 5 patients) were performed to incorporate the ISCEV Standards.[21,22] ERGs were recorded under dark-adapted (DA) conditions to flash strengths of 0.01 and 10.0 cd.s.m^{-2}; light-adapted (LA) ERGs to flash strength of 3.0 cd.s.m^{-2} (30Hz and 2Hz). An additional larger field PERG (30º x24º) was recorded in

2 patients as previously described.[23]

Molecular investigation

Genomic DNA was isolated from peripheral blood lymphocytes using the Puregene kit (Gentra Puregene Blood Extraction Kit, QIAGEN, Manchester, UK). Whole exome sequencing was performed on patients 1-5 and 9 as part of the National Institute for Health Research (NIHR) BioResource funded Specialist Pathology: Evaluating Exomes in Diagnostics (SPEED) study (Cambridge Biomedical Centre, UK). As part of this study, more than 600 unrelated patients from Moorfields Eye Hospital and Great Ormond Street Hospital with a range of inherited retinal diseases underwent whole-exome sequencing or whole-genome sequencing with patients 1-5 and 9 all from the exome cohort. Exome enrichment was performed using ROCHE NimbleGen SeqCap EZ 64 Mb Human Exome Library version 3.0 (ROCHE NimbleGen, Inc., Madison, WI, USA). The libraries were sequenced on an Illumina HiSeq 2000. Reads were aligned to the GRCh37 reference genome using novoalign version 2.08.03. Duplicate reads were marked using Picard tools MarkDuplicates. Calling was performed using the haplotype caller module of GATK (https://www.broadinstitute.org/gatk, version 3.3-0), creating gVCF formatted files for each sample. The individual gVCF files for the exomes discussed in this study, in combination with approximately 3,000 clinical exomes (University College London exomes consortium), were combined into merged VCF files for each chromosome containing on average 100 samples each. The final variant calling was performed using the GATK GenotypeGVCFs module jointly for all samples (cases and controls). Variant quality scores were then re-calibrated according to GATK best practices separately for indels and SNPs. Resulting variants were annotated using ANNOVAR based on Ensembl gene and transcript definitions. Candidate variants were filtered based on function (non synonymous, presumed loss-of-function or splicing, defined as intronic sites within 5 bp of an exon-intron junction) and minor allele frequency (< 0.5% minor allele frequency in our

internal control group, as well as the NHLBI GO Exome Sequencing Project dataset, EVS, available at http://evs.gs.washington.edu/EVS/).

Next generation sequencing of the coding regions of 105 genes for patients 7 and 8 and more recently for 176 retinal genes for patient 10 was performed at the Manchester Centre for Genomic Medicine (Manchester, UK) with enrichment using a SureSelect Target Enrichment Kit (Agilent Technologies Inc., Santa Clara, USA) then run on a SOLiD 4 sequencer (Life Technologies, Grant Island, NY, USA).[24] More then 500 unrelated patients with a range of inherited retinal dystrophies recruited from Moorfields Eye Hospital have undergone this molecular investigation.

Confirmatory bi-directional Sanger sequencing of *CNGB1* was performed in all probands and available family members. DNA was amplified using specifically designed primers by polymerase chain reaction (PCR) and the resulting fragments sequenced using standard protocols.

Variant nomenclature was assigned in accordance with GenBank Accession number NM_001297.4 with nucleotide position 1 corresponding to the A of the ATG initiation codon. Variants were identified as novel if not previously reported in the literature and if absent from dbSNP (available at http://www.ncbi.nlm.nih.gov/projects/SNP/); EVS; and the Exome Aggregation Consortium database (ExAC, available at http://exac.broadinstitute.org) containing 61,486 exomes, all accessed 21st March 2016. Where relevant, potential splice site disruption was assessed using Splice Site Prediction by Neural Network (available at http://www.fruitfly.org/seq_tools/splice.html).

Results

Clinical Evaluation

The series consisted of 10 patients (7 females and 3 males). Eight were Caucasian British, one Bangladeshi (patient 4) and one Afghani (patient 9). The clinical findings are summarized in Table 1, with family pedigrees and identified variants shown in Figure 1. Mean age at last review was

47.4 ± 13.2 years (range 15-65) with a mean follow-up of 3.7 ± 2.8 years (range 0-11). The initial symptom in all patients was nyctalopia with onset from infancy to 14 years of age. No patient reported photophobia. A fine nystagmus was observed in one patient (patient 9). Symptomatic peripheral visual field loss occurred later, at a mean age of 33.2 ± 8.0 years (range 13-40), although it was detectable on formal kinetic perimetry in patient 9 at age 12 years. Six of 10 patients developed visually significant posterior subcapsular lens opacities in both eyes during follow-up with subsequent cataract surgery.

Mean BCVA was 0.1 LogMAR (20/25 Snellen) in the right eye (range 0 to 0.3, Snellen 20/20 to 20/40) and 0.1 LogMAR in the left eye (range -0.1 to 0.3, Snellen 20/16 to 20/40). Myopic refractive errors were present in three of the patients for whom data were available. Confrontation visual field testing demonstrated variable peripheral field loss in all subjects. There was sparing of the central 20-30 degrees in 7 patients; sparing of the central 10-20 degrees in 1 patient; and sparing of the central 5-10 degrees in 2 patients, with documented slow progression during follow-up.

Fundus examination of all but patient 9, revealed arteriolar attenuation, optic disc pallor, retinal pigment epithelium (RPE) atrophy and mid-peripheral intra-retinal pigment migration. For patient 9, the youngest patient, narrow retinal vessels and mid-peripheral RPE mottling were the only observable abnormalities at age 18 years. (Figure 2) Peri-foveal RPE atrophy was additionally present in patients 1, 4 and 10.

FAF imaging showed a loss of autofluorescence in the mid-periphery with macular or perimacular rings of increased autofluorescence in all patients. Patient 9 with initial preserved autofluorescence developed a macular ring of increased autofluorescence over a 5-year follow up period (Figure 2). Three patients (patients 1, 4 and 10), had an additional patchy peri-foveal ring of reduced autofluorescence corresponding to their peri-foveal RPE atrophy.

One patient with a large paracentral ring of FAF had complete preservation of the inner segment ellipsoid (ISe) band evident on OCT (Figure 2, patient 8). In others the lateral extent of the ISe band corresponded with the diameter of the ring of increased signal on FAF with the most severe loss of

ISe band in patients 1 and 10. In addition, both eyes of patient 3, 6 and the left eye of patient 7 had an epiretinal membrane; patient 5 had bilateral vitreomacular traction (VMT) associated with macular edema and patient 10 a small left lamellar macular hole without apparent VMT. Interval OCT imaging over a 5 year period in patient 9 demonstrated a marked reduction in the diameter of the ISe band (Figure 2). Mean CST thickness, excluding patient 5 (macular edema) and patient 9 (information unavailable), was 302.3 μm ± 35.0 μm in the right eye and 295.3 ± 33.0 μm in the left eye compared to mean normative values of 270.2 ± 22.5 μm.[25] Excluding those patients with all concurrent macular pathology resulted in similar values for the CST for patients 1, 2, 4, 7 (RE), 8 and 10 (RE) of 297.7 ± 37.1 μm in the right eye and 291.8 ± 42.8 μm in the left eye.

Full-field ERG and PERG were performed in 6 patients at the mean age of 40 ± 13.2 years old. Full-field ERG performed in patient 9 at the age of 13 years old showed profoundly attenuated rod-specific responses (dark-adapted 0.01) with subnormal and delayed cone responses. In the other 5 patients, rod-specific responses (dark-adapted 0.01) were undetectable bilaterally; the brighter flash dark-adapted ERGs (dark-adapted 3.0 and dark-adapted 10.0) showed markedly reduced or undetectable function from both eyes (figure 3). Light-adapted 30Hz flicker ERGs and single-flash cone ERG b-waves were delayed and subnormal in most, subnormal without delay in patient 8 and with only a residual single flash cone ERG detectable in patient 7. The PERG P50 responses in 5 patients ranged from undetectable to normal (table 1, figure 3). Patients 7 and 8 underwent large field PERG testing with lack of enlargement of the response for patient 7 indicating marked paracentral retinal dysfunction and the expected enlargement relative to the standard PERG for patient 8 indicating relative preservation of paracentral macular function (figure 3).

CNGB1 **Screening**

Likely pathogenic variants in *CNGB1* were identified in all 9 probands and, after segregation analysis, in a further 3 affected family members, one of whom was also available for examination (patient 6). One previously reported variant, c.2957A>T (p.(N986I)) in exon 29, was identified in

patients 2, 3, 5, 7 and 8 (Figure 1).[16] Four novel variants were detected; 3 nonsense, c.262C>T (p.(Q88*)) in exon 3, c.664C>T (p.(Q222*)) in exon 10, c.2185C>T (p.(R729*)) in exon 22 and one splice site variant c.761+2T>A in intron 10 predicted to abolish the canonical splice donor site. These were all absent from the ExAC database. In addition 3 variants were detected not previously reported in an affected patient before but present at a very low allele frequency in the ExAC database; c.952C>T (p.(Q318*)) in exon 13 (1/120768 alleles), c.3142_3143insGTGG (p.(A1048fs*13)) in exon 31 (2/120522 alleles) and c.2544dupG (p.(L849Afs*3)) in exon 26 (4/120644 alleles). For patient 3 (GC19136) and patients 5-6 (GC635), further segregation to establish phase was not possible from either antecedents or children; however the 2 variants found did segregate with additional affected individuals in both families (Figure 1).

Discussion

This report describes the findings in 10 patients (7 female, 3 male) from 9 families with a typical RP phenotype and likely pathogenic variants in *CNGB1*. Seven likely pathogenic variants not previously reported in an affected patient were identified.

There are limited published data of the *CNGB1* retinal phenotype.[10,15-20] To our knowledge, only 7 families have been identified with recessive RP due to *CNGB1* comprising 3 missense variants, 3 splice site variants and 1 frameshift variant. Of the 4 families with clinical detail, there was a childhood onset of nyctalopia with a later development of peripheral visual field loss reported in 4 patients at ages 10, 20 and 30 (2 patients) years.[10,15,17,19] Severe loss of visual acuity was present in 3 patients at age 24, 57 and 67 years. There were fundus abnormalities typical of RP with mid-peripheral RPE atrophy and intra-retinal bone-spicule pigmentation and variable macular atrophy. Two patients had undetectable rod responses on ERG and severely abnormal cone responses aged 24 and 30 years; 1 patient had undetectable ERG responses at age 44 years. PERG was not performed. The patients in the present series had similar features; onset of nyctalopia was in childhood with symptomatic visual field loss occurring later; central visual acuity was preserved

well into adult life; there were fundus abnormalities consistent with RP; and electrophysiology demonstrated a rod-cone dystrophy phenotype. Pattern ERGs showed variable degrees of central or paracentral macular involvement and could be relatively preserved in patients with ERG evidence of severe generalized photoreceptor dysfunction.

This is the first report to describe retinal imaging (other than fundus appearance); all patients demonstrated reduced mid-peripheral autofluorescence with macular rings of increased autofluorescence corresponding to the size of remaining ISe band. Abnormal para-foveal rings of increased FAF have been reported in approximately 59% of RP patients. [26] All patients in the present series demonstrated such abnormal rings, the largest FAF ring surrounded an area that included most of the vascular arcades in a patient with OCT evidence of preserved outer retina (patient 8, figure 2) and relatively preserved PERG (figure 3). The diameter of smaller FAF rings corresponded with the lateral limit of the remaining OCT ISe band, consistent with previous studies of RP patients that have shown spatial correspondence or correlation between these parameters.[27,28] Central subfield thickness was within normal limits. The findings of our study suggest that RP associated with variants in *CNGB1* has a good prognosis for central vision despite the early onset of night blindness. The good visual prognosis is reflected by preserved central macular thickness and morphology of the inner segment ellipsoid band of the photoreceptors even in adult patients.

A total of 8 different variants in *CNGB1* were identified. The previously reported missense variant, p.(N986I), was detected in 5 patients, all British Caucasian, suggesting it to be a common *CNGB1* variant in this population.[16] It is found in 133/120,752 alleles with no homozygotes in the ExAC database (minor allele frequency, MAF 0.0011), including 84/66,728 non-Finnish European alleles (MAF 0.0013). Patient 1, bi-allelic for nonsense variants, had a more severe phenotype compared to the other patients; the BCVA was 0.3 LogMAR (Snellen 20/40) at age of 47 years old and the visual field was restricted to the central 10 degrees in both eyes. This patient is predicted nullizygous for *CNGB1* due to nonsense mediated decay of the transcribed mRNA as are patients 4, 9 and 10 suggesting that there is no direct correlation between predicted nullizygous variants and

phenotype severity.[29] Of the previously reported patients with clinical detail, 2 had splice site variants (c.413-1G>A and c.3444+1G>A) and visual loss at ages 24 and 67 years respectively; 2 with missense variants had preserved central vision in to at least their 4th decades.[10,15,17,19] The splice site variants have both been shown *in vitro* to lead to aberrant splicing and premature termination codons.[19,30] At this time, there is no demonstrable genotype-phenotype correlation. Further functional work and larger numbers of patients may help elucidate potential associations.

The slowly progressive RP phenotype in *CNGB1* patients is consistent with the prior canine and murine model studies.[31,32,33] In Papillon dogs with a homozygous frameshift variant in *CNGB1*, there was marked reduction or absence of rod ERG responses with a partial preservation of cone ERGs.[31] OCT imaging of the central macula, when fully developed (approximately 8 weeks of age), showed retinal layer thickness comparable to a normal control with a gradually progressive thinning of the outer nuclear layer with age, confirming a slow retinal degeneration. In *Cngb1*$^{-/-}$ mice, a progressive loss of rod photoreceptor function was noted with a later degeneration of cone photoreceptors.[32] The degeneration was slow with loss of 20-30% of rods at 4 months, 30-50% at 6 months and 80-90% at 1 year. Although the rods degenerated early, cone photoreceptors started to degenerate only at 6 months, and were still present at 11 months.[32,33]

To conclude, this report exparvnds the phenotype of patients with RP due to variants in *CNGB1* and describes 7 additional pathogenic variants. The phenotype, similar to previous reports and animal models, indicates slow degeneration and there is therefore a lengthy window of opportunity for therapeutic intervention. The results from proof of concept gene therapy studies in a *Cngb1* knockout mouse model leads to optimism that human RP associated with variants in *CNGB1* may ultimately be treated successfully using a similar approach.[34]

ACKNOWLEDGMENTS

The authors would like to acknowledge the National Institute for Health Research BioResource-Rare Diseases consortium for the molecular investigations performed in this report as part of the UK national SPEED study.

Financial disclosures/conflicts of interest: The authors have no proprietary or commercial interest in any materials discussed in this article. No conflicting relationship pertinent to the subject matter or materials discussed in this paper exists for any author.

Funding Sources: The National Institute for Health Research (NIHR) England for supporting the NIHR BioResource–Rare Diseases and Biomedical Research Centres at Moorfields Eye Hospital and the UCL Institute of Ophthalmology; The Foundation Fighting Blindness; Fight For Sight; Moorfields Eye Hospital Special Trustees; Rosetrees Trust; Research to Prevent Blindness USA.

Funding bodies did not have any specific role in the design and conduct of the study; collection, management, analysis, and interpretation of the data; preparation, review, or approval of the manuscript; nor decision to submit the manuscript for publication.

Access to data statement: SH and MA had full access to all of the data in this study and takes responsibility for the integrity of the data and the accuracy of the data analysis.

Author contributions: SH, MA and AW designed the study; all authors acquired, analyzed or interpreted data; SH and MA drafted the manuscript; all authors critically revised the manuscript for important intellectual content.

References

1. Fahim AT, Stephen PWeleber, Richard G. *Retinitis Pigmentosa Overview.* Seattle: University of Washington; 2013.
2. Wang DY, Chan WM, Tam PO, et al. Gene mutations in retinitis pigmentosa and their clinical implications. *Clin Chim Acta.* 2005;351(1-2):5-16.
3. Jacobson SG, Voigt WJ, Parel JM, et al. Automated light- and dark-adapted perimetry for evaluating retinitis pigmentosa. *Ophthalmology.* 1986;93(12):1604-1611.

4. Hartong DT, Berson EL, Dryja TP. Retinitis pigmentosa. *Lancet.* 2006;368(9549):1795-1809.
5. Fishman GA. Retinitis pigmentosa. Genetic percentages. *Arch Ophthalmol.* 1978;96(5):822-826.
6. Hims MM, Diager SP, Inglehearn CF. Retinitis pigmentosa: genes, proteins and prospects. *Dev Ophthalmol.* 2003;37:109-125.
7. Bocquet B, Lacroux A, Surget MO, et al. Relative frequencies of inherited retinal dystrophies and optic neuropathies in Southern France: assessment of 21-year data management. *Ophthalmic Epidemiol.* 2013;20(1):13-25.
8. Dryja TP, Finn JT, Peng YW, McGee TL, Berson EL, Yau KW. Mutations in the gene encoding the alpha subunit of the rod cGMP-gated channel in autosomal recessive retinitis pigmentosa. *Proc Natl Acad Sci U S A.* 1995;92(22):10177-10181.
9. Tanackovic G, Ransijn A, Ayuso C, Harper S, Berson EL, Rivolta C. A missense mutation in PRPF6 causes impairment of pre-mRNA splicing and autosomal-dominant retinitis pigmentosa. *Am J Hum Genet.* 2011;88(5):643-649.
10. Bareil C, Hamel CP, Delague V, Arnaud B, Demaille J, Claustres M. Segregation of a mutation in CNGB1 encoding the beta-subunit of the rod cGMP-gated channel in a family with autosomal recessive retinitis pigmentosa. *Hum Genet.* 2001;108(4):328-334.
11. Biel M, Michalakis S. Function and dysfunction of CNG channels: insights from channelopathies and mouse models. *Mol Neurobiol.* 2007;35(3):266-277.
12. Kaupp UB, Seifert R. Cyclic nucleotide-gated ion channels. *Physiol Rev.* 2002;82(3):769-824.
13. Zheng J, Trudeau MC, Zagotta WN. Rod cyclic nucleotide-gated channels have a stoichiometry of three CNGA1 subunits and one CNGB1 subunit. *Neuron.* 2002;36(5):891-896.
14. Peng C, Rich ED, Varnum MD. Subunit configuration of heteromeric cone cyclic nucleotide-gated channels. *Neuron.* 2004;42(3):401-410.
15. Kondo H, Qin M, Mizota A, et al. A homozygosity-based search for mutations in patients with autosomal recessive retinitis pigmentosa, using microsatellite markers. *Invest Ophthalmol Vis Sci.* 2004;45(12):4433-4439.
16. Simpson DA, Clark GR, Alexander S, Silvestri G, Willoughby CE. Molecular diagnosis for heterogeneous genetic diseases with targeted high-throughput DNA sequencing applied to retinitis pigmentosa. *J Med Genet.* 2011;48(3):145-151.
17. Bocquet B, Marzouka NA, Hebrard M, et al. Homozygosity mapping in autosomal recessive retinitis pigmentosa families detects novel mutations. *Mol Vis.* 2013;19:2487-2500.
18. Maria M, Ajmal M, Azam M, et al. Homozygosity mapping and targeted sanger sequencing reveal genetic defects underlying inherited retinal disease in families from pakistan. *PLoS One.* 2015;10(3):e0119806.
19. Saqib MA, Nikopoulos K, Ullah E, et al. Homozygosity mapping reveals novel and known mutations in Pakistani families with inherited retinal dystrophies. *Sci Rep.* 2015;5:9965.
20. Maranhao B, Biswas P, Gottsch AD, et al. Investigating the Molecular Basis of Retinal Degeneration in a Familial Cohort of Pakistani Decent by Exome Sequencing. *PLoS One.* 2015;10(9):e0136561.
21. McCulloch DL, Marmor MF, Brigell MG, et al. ISCEV Standard for full-field clinical electroretinography (2015 update). *Doc Ophthalmol.* 2015;130(1):1-12.
22. Bach M, Brigell MG, Hawlina M, et al. ISCEV standard for clinical pattern electroretinography (PERG): 2012 update. *Doc Ophthalmol.* 2013;126(1):1-7.
23. Lenassi E, Robson AG, Hawlina M, Holder GE. The value of two-field pattern electroretinogram in routine clinical electrophysiologic practice. *Retina.* 2012;32(3):588-599.
24. O'Sullivan J, Mullaney BG, Bhaskar SS, et al. A paradigm shift in the delivery of services for diagnosis of inherited retinal disease. *J Med Genet.* 2012;49(5):322-326.
25. Grover S, Murthy RK, Brar VS, Chalam KV. Normative data for macular thickness by high-definition spectral-domain optical coherence tomography (spectralis). *Am J Ophthalmol.* 2009;148(2):266-271.
26. Murakami T, Akimoto M, Ooto S, et al. Association between abnormal autofluorescence and photoreceptor disorganization in retinitis pigmentosa. *Am J Ophthalmol.* 2008;145(4):687-694.
27. Robson AG, Tufail A, Fitzke F, et al. Serial imaging and structure-function correlates of high-density rings of fundus autofluorescence in retinitis pigmentosa. *Retina.* 2011;31(8):1670-1679.

28. Greenstein VC, Duncker T, Holopigian K, et al. Structural and functional changes associated with normal and abnormal fundus autofluorescence in patients with retinitis pigmentosa. *Retina.* 2012;32(2):349-357.
29. Lejeune F, Maquat LE. Mechanistic links between nonsense-mediated mRNA decay and pre-mRNA splicing in mammalian cells. *Curr Opin Cell Biol.* 2005;17(3):309-315.
30. Becirovic E, Nakova K, Hammelmann V, Hennel R, Biel M, Michalakis S. The retinitis pigmentosa mutation c.3444+1G>A in CNGB1 results in skipping of exon 32. *PLoS One.* 2010;5(1):e8969.
31. Winkler PA, Ekenstedt KJ, Occelli LM, et al. A large animal model for CNGB1 autosomal recessive retinitis pigmentosa. *PLoS One.* 2013;8(8):e72229.
32. Hüttl S, Michalakis S, Seeliger M, et al. Impaired channel targeting and retinal degeneration in mice lacking the cyclic nucleotide-gated channel subunit CNGB1. *J Neurosci.* 2005;25(1):130-138.
33. Zhang Y, Molday LL, Molday RS, et al. Knockout of GARPs and the β-subunit of the rod cGMP-gated channel disrupts disk morphogenesis and rod outer segment structural integrity. *J Cell Sci.* 2009;122(Pt 8):1192-1200.
34. Michalakis S, Koch S, Sothilingam V, et al. Gene therapy restores vision and delays degeneration in the CNGB1(-/-) mouse model of retinitis pigmentosa. *Adv Exp Med Biol.* 2014;801:733-739.

Table 1. Summary of Clinical Findings in *CNGB1* patients.

Patient (family)	Age at last review, years	Length review, years	Age of onset (symptoms)	Latest BCVA		Visual Field to confrontation	OCT	Age in years at electrophysiology, findings
				RE	LE			
1 (GC2533)	54	4	8yrs (*night blindness)* 30yrs (*loss of peripheral vision)*	0.3 (20/40)	0.3 (20/40)	5°-10° central	Centrally preserved ISe band	Not performed
2 (GC20388)	40	-	childhood (*night blindness)* 30yrs (*loss of peripheral vision)*	0.3 (20/40)	0.2 (20/32)	20°-30° central	Centrally preserved ISe band	Not performed
3 (GC19136)	55	3	childhood (*night blindness)* 40yrs (*loss of peripheral vision)*	0.0 (20/20)	-0.1 (20/16)	20°-30° central	Centrally preserved ISe band BE ERM	Subnormal PERG; undetectable rod ERG, subnormal cone ERG (ERG performed and reported elsewhere)
4 (GC19695)	50	4	childhood (*night blindness)* 39yrs (*loss of peripheral vision)*	0.0 (20/20)	-0.1 (20/16)	20°-30° central	Centrally preserved ISe band	38, subnormal RE PERG, normal LE PERG; undetectable rod ERG, subnormal bright flash ERG; subnormal & delayed cone ERGs
5 (GC635)	65	3	childhood (*night blindness)* 38yrs (*loss of peripheral vision)*	0.2 (20/32)	0.2 (20/32)	20°-30° central	Centrally preserved ISe band BE CMO BE VMT	53, undetectable PERG; undetectable rod ERG; subnormal bright flash ERG; delayed & subnormal cone ERGs
6 (GC635)	60	4	childhood (*night blindness)* 40yrs (*loss of peripheral vision)*	0.0 (20/20)	-0.1 (20/16)	10°-20° central	Centrally preserved ISe band	Not performed
7 (GC20934)	43	1	childhood (*night blindness)* 40yrs (*loss of peripheral vision)*	0.0 (20/20)	0.0 (20/20)	20°-30° central	Centrally preserved ISe band LE ERM	42, subnormal PERG; undetectable rod ERG; undetectable bright flash and flicker ERG; residual single flash cone ERG
8 (GC21053)	40	2	childhood (*night blindness)* 32yrs (*loss of peripheral vision)*	0.2 (20/32)	0.2 (20/32)	30° central	ISe band preserved throughout macula	39, subnormal PERG; undetectable rod ERG, subnormal bright flash ERG, subnormal cone ERGs.

9	18	5	infancy *(night blindness)* 13 yrs (*loss of peripheral vision)*	0.1 (20/25)	0.1 (20/25)	25°-30° central	Centrally preserved ISe band	13, PERG not performed; profoundly attenuated rod ERGs, subnormal & delayed cone ERGs
10 (GC17300)	49	11	childhood *(night blindness)* 30yrs (*loss of peripheral vision)*	0.0 (20/20)	0.18 (20/30)	5°-10° central	Centrally preserved ISe band LE LMH	Not performed

455 BE, both eyes; RE right eye; LE left eye; BCVA best corrected visual acuity LogMAR (Snellen); OCT
456 optical coherence tomography; PERG pattern electroretinography; ERG electroretinography; ERM epiretinal
457 membrane; ISe, inner segment ellipsoid; CMO cystoid macular edema, VMT vitreomacular traction, LMH
458 lamellar macular hole

459

460 **Figure legends**

461

462 **Figure 1**

463 **Title: Pedigrees of 9 families with variants**

464

465 **Figure 2**

466 **Title: Retinal imaging in *CNGB1* related retinal dystrophy**

467 Color fundus photographs, fundus autofluorescence (FAF) imaging and optical coherence
468 tomography (OCT) for patients 3, 4, 5, 8 and 9. (A) patient 3, (B) patient 4 and (C) patient 5, all
469 right eye (RE): mid-peripheral retinal pigment epithelium (RPE) atrophy with bone spicule
470 hyperpigmentation, reduced autofluorescence in mid-periphery with ring of increased macula
471 autofluorescence corresponding to preserved inner segment ellipsoid (ISe) band on OCT; patient 3
472 epiretinal membrane also present on OCT; patient 4 reduced peri-foveal dots of autofluorescence
473 also present; patient 5 vitreomacular traction with retinal cysts of inner nuclear layer also present on
474 FAF imaging and OCT. (D) patient 8 left eye (LE), mid-peripheral RPE atrophy and pigmentary
475 change as before but with a large ring of increased autofluorescence outside of the macula on FAF

imaging, anterior to which reduced autofluorescence is present, and on OCT imaging, preserved retinal layers. (E) patient 9 RE and LE color fundus imaging from 2011 demonstrates narrowing of the vessels only, FAF imaging normal in 2011 but in 2016, rings of increased autofluorescence present in both eyes, partially preserved ISe band in 2011 with reduction in size demonstrated in 2016

Figure 3

Title: **Electroretinography in *CNGB1* related retinitis pigmentosa.** Full-field and pattern ERGs in patients 4 (age 38 years), 5 (age 53 years), 7 (age 42 years) and 8 (age 39 years) and traces from a representative normal subject for comparison. The ERGs showed a high degree of interocular symmetry and are shown for one eye only; responses are consistent with rod-cone dystrophy. PERG was normal in one eye of case 4 (mildly subnormal in the other eye; data not shown) and showed reduction indicating symmetrical mild-severe macular dysfunction in the other patients.

Patient 1 (GC2533)
M1: c.262C>T (p.(Q88*))
M2:c.664C>T (p.(Q222*))

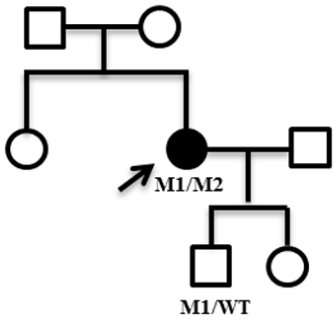

Patient 2 (GC20388)
M: c.2957A>T (p.(N986I))

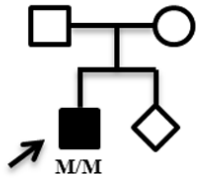

Patient 3 (GC19136)
M1: c.2957A>T (p.(N986I))
M2: c.3142_3143insGTGG (p.(A1048fs*13))

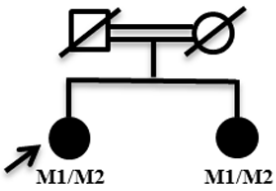

Patient 4 (GC19695)
M: c.761+2T>A

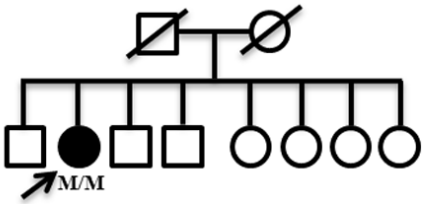

Patient 5 - Patient 6* (GC635)
M1: c.952C>T (p.(Q318*))
M2: c.2957A>T (p.(N986I))

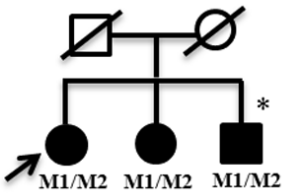

Patient 7 (GC20934)
M: c.2957A>T (p.(N986I))

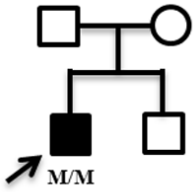

Patient 8 (GC21053)
M: c.2957A>T (p.(N986I))

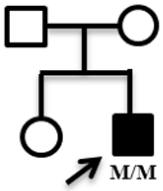

Patient 9
M: c.2185C>T (p.(R729*))

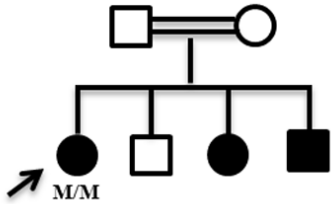

Patient 10 (GC17300)
M: c.2544dupG (p.(L849Afs*3))

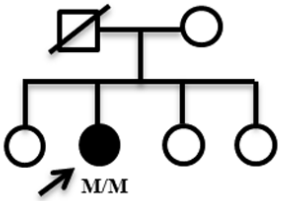

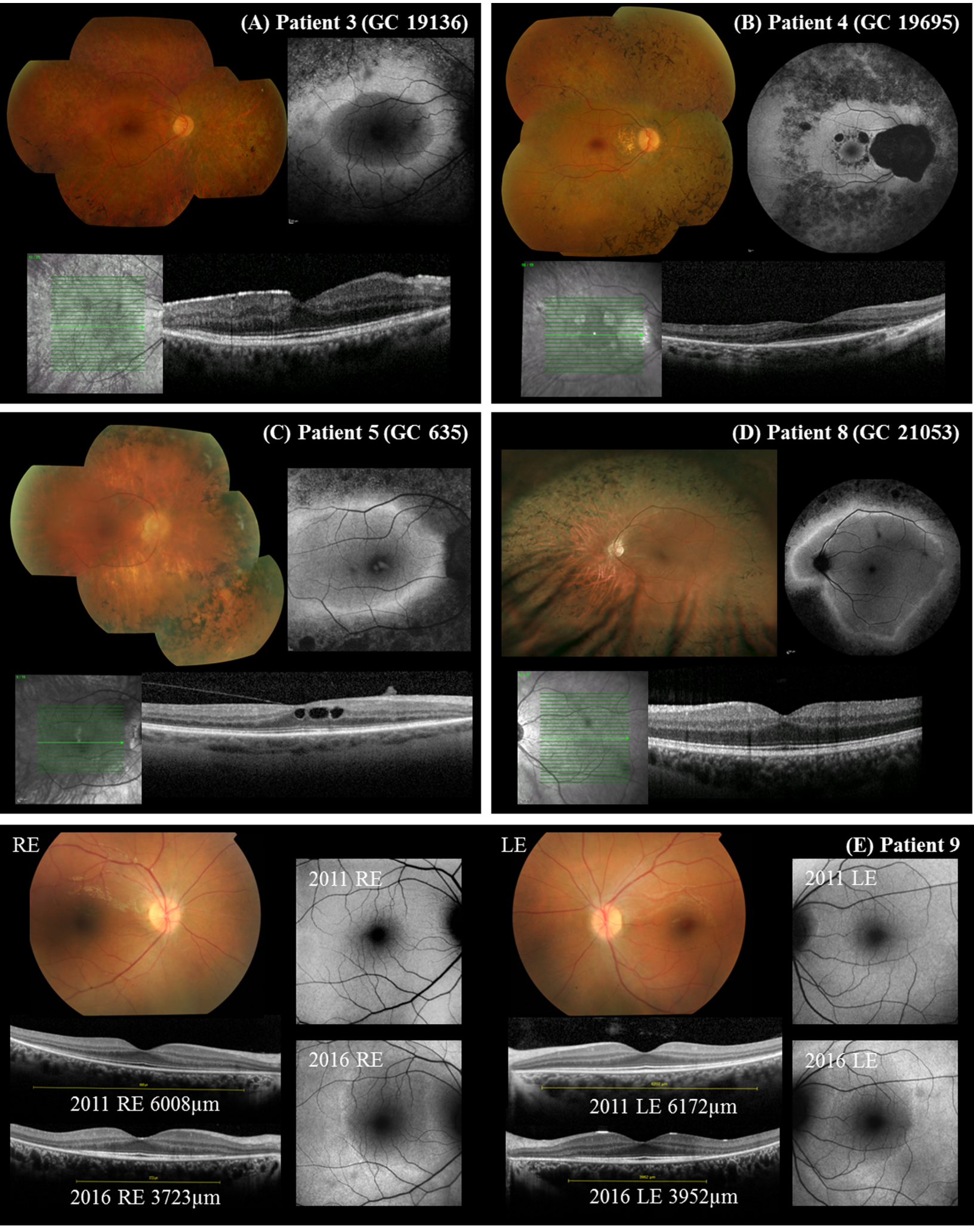
(A) Patient 3 (GC 19136)
(B) Patient 4 (GC 19695)
(C) Patient 5 (GC 635)
(D) Patient 8 (GC 21053)
RE
2011 RE
2016 RE
2011 RE 6008µm
2016 RE 3723µm
LE
(E) Patient 9
2011 LE
2016 LE
2011 LE 6172µm
2016 LE 3952µm

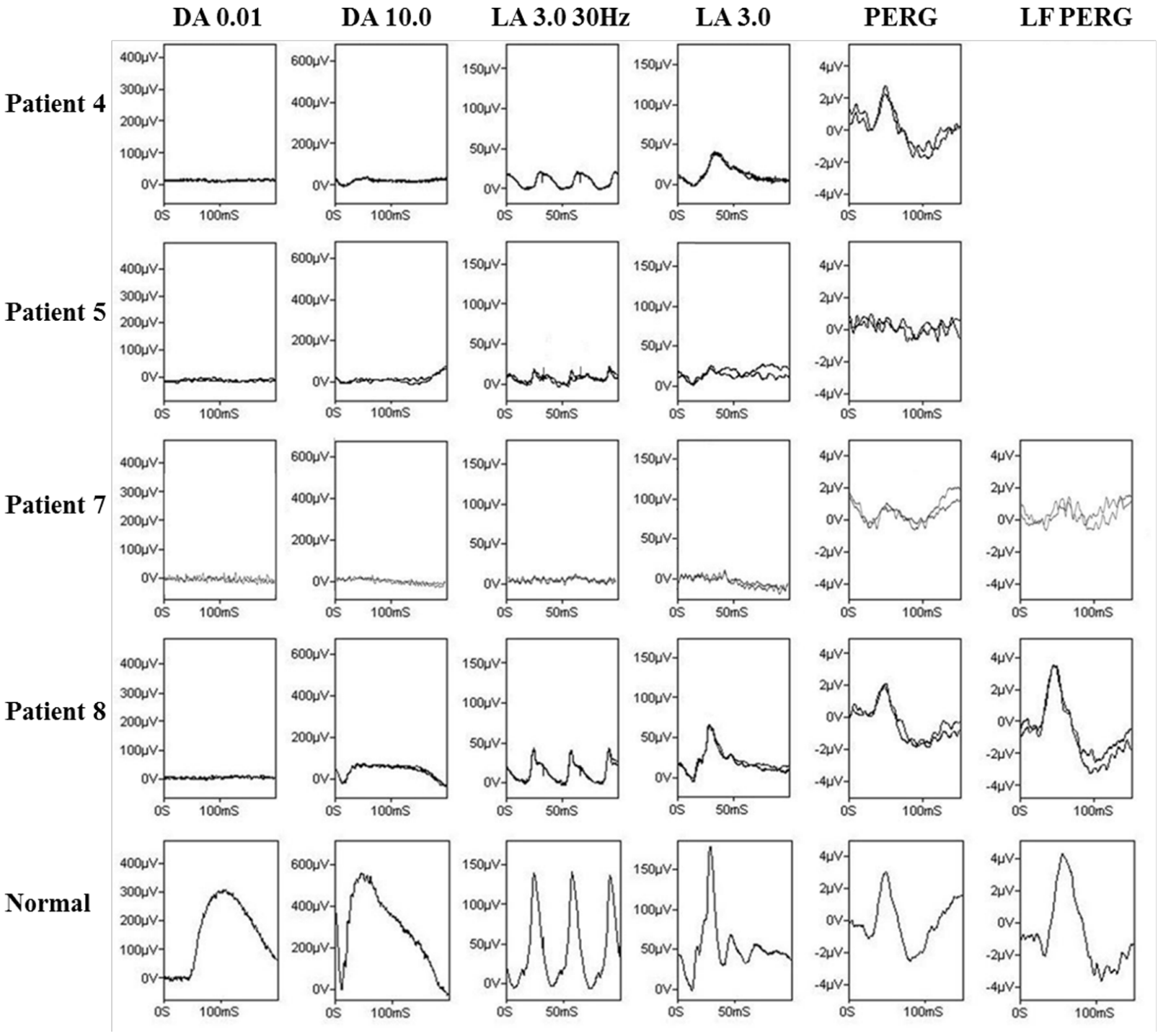
DA 0.01
DA 10.0
LA 3.0 30Hz
LA 3.0
PERG
LF PERG
Patient 4
Patient 5
Patient 7
Patient 8
Normal
400µV
300µV
200µV
100µV
0V
600µV
150µV
50µV
4µV
2µV
-2µV
-4µV
0S
100mS
50mS